PHYSICAL REVIEW D **72,** 105007 (2005)

Testing CPT symmetry with supernova neutrinos

Hisakazu Minakata* and Shoichi Uchinami†

Department of Physics, Tokyo Metropolitan University, 1-1 Minami-Osawa, Hachioji, Tokyo 192-0397, Japan

(Received 20 May 2005; revised manuscript received 15 August 2005; published 11 November 2005)

Diagnosing the core of supernova requires favor-dependent reconstruction of three species of neutrino spectra, ν_e, $\bar{\nu}_e$, and ν_x (a collective notation for ν_μ, $\bar{\nu}_\mu$, ν_τ, and $\bar{\nu}_\tau$). We point out that, assuming the information is available, CPT symmetry can be tested with supernova neutrinos. We classify all possible level crossing patterns of neutrinos and antineutrinos into six cases and show that half of them contains only the CPT-violating mass and mixing patterns. We discuss how additional information from terrestrial experiments helps in identifying CPT violation by narrowing down the possible flux patterns. Although the method may not be a good precision test, it is particularly suited for uncovering gross violation of CPT such as different mass patterns of neutrinos and antineutrinos. The power of the method is due to the nature of the level crossing in supernova which results in the sensitivity to neutrino mass hierarchy and to the unique characteristics of *in situ* preparation of both ν and $\bar{\nu}$ beams. Implications of our discussion to the conventional analyses with CPT invariance are also briefly mentioned.

DOI: 10.1103/PhysRevD.72.105007 PACS numbers: 11.30.Er, 14.60.Pq, 97.60.Bw

I. INTRODUCTION

CPT is one of the most fundamental symmetries in relativistic quantum field theory [1], by which masses and flavor mixing angles are constrained to be identical for particles and their antiparticles. Because of the fundamental nature of the symmetry, it is important to test the CPT invariance and there have been continuing efforts mainly in kaon physics [2]. Needless to say, the effort of testing CPT symmetry should be extended to the lepton sector.

Recently, there arose some interest in possible violation of CPT symmetry in the lepton sector, partly motivated by a possible interpretation of the LSND result [3]. An hypothesis of different mass and mixing patterns of neutrino and antineutrino sectors, as first suggested by Murayama and Yanagida [4], could be flexible enough to accommodate the LSND data in the three-neutrino framework, while not sacrificing the success of describing the atmospheric, the solar, the reactor, and the accelerator data [5–8]. While the proposal was followed by a series of papers [9–11], it was shown by Gonzalez-Garcia, Maltoni, and Schwetz [12], in an extensive statistical analysis of all the data including KamLAND [7], that the CPT-violating hypothesis is not in good shape. Interestingly, the best fit point of all data except for LSND is CPT symmetric, and the mixing parameter region favored by LSND is more than 3σ away from the region favored by all but LSND data.

In this paper, we explore the possibility of testing CPT symmetry with supernova neutrinos. Independent of the success or the failure of the CPT-violating scenario for the LSND data, it is important to test CPT as a fundamental symmetry in nature. Given the fact that neutrinos have brought us several surprises, there exists an even more intriguing (albeit not likely) possibility to discover CPT violation by future neutrino experiments. Supernova neutrinos are advantageous to examine neutrino and antineutrino properties simultaneously and consistently because the beam is composed not only of ν_e, ν_μ, and ν_τ but also their antiparticles. We examine the possibility of using neutrinos from supernova to identify CPT violation assuming the resolving power of flavor-dependent neutrino fluxes in a future observation of galactic supernovae.

So far, constraints on CPT violation of mixing parameters in the lepton sector have been derived by the Super-Kamiokande (SK) group [13] and in [12]. Possible ways of testing CPT symmetry have been discussed by using solar and reactor neutrinos [14,15] and a neutrino factory [16]. We restrict ourselves, as these preceding works do, to the framework of possible CPT violation in masses and flavor mixing of neutrinos, assuming that neutrino interactions conserve CPT. Then, the natural question is how the supernova method can be competitive to these more ''traditional'' methods for testing CPT. It is the right question because it is unlikely that such a rare event as supernova can be used for a precision test of CPT symmetry. Despite the reasonable skepticism, we will show in this paper that the supernova neutrino can be a powerful tool for uncovering a gross violation of CPT symmetry. (See Sec. II for further comments.)

We rely on Ref. [17] for the formulas of neutrino flavor conversion in supernova in the three-flavor framework. We should note that our general CPT noninvariant treatment, of course, includes the case of CPT invariance. Therefore, the reader can use part of the formulas given in this paper as a compact recollection of those in [17], but by now without ambiguities due to the solar neutrino solutions.

In Sec. II, we discuss the question of why and how supernova neutrinos are useful to test CPT. In Sec. III, we review the basic properties of supernova neutrinos and the approximations involved in our treatment. In

*Electronic address: minakata@phys.metro-u.ac.jp
†Electronic address: uchinami@phys.metro-u.ac.jp

Sec. IV, after recollecting compact formulas for neutrino flavor conversion in supernova, we present a complete classification of spectral patterns of supernova neutrinos that are possible in a general CPT-violating ansatz. In Sec. V, we discuss how the allowed flux patterns of supernova neutrinos reduce as additional input of θ_{13} and neutrino mass hierarchy is added. In Sec. VI, we give a comparative study of characteristic features of spectra of three effective neutrino species predicted in each classified pattern of neutrino flavor transformation in supernova. In Sec. VII, we discuss at a qualitative (or semiquantitative) level to what extent the possible different neutrino flux patterns can be discriminated observationally. In Sec. VIII, we give the concluding remarks.

II. WHY AND HOW ARE SUPERNOVA NEUTRINOS USEFUL TO TEST CPT?

To answer the question of why and how supernova neutrinos are useful to test CPT we need to specify the question: Namely, which aspects of CPT symmetry do we want to test, or which features of CPT violation do we want to try to uncover?

First of all, lacking well-defined models of CPT violation, we cannot test CPT in neutrino interactions by using supernova neutrinos. If the interactions are different from what we know the neutrino properties inside the core must be recomputed with new interactions to define CPT noninvariant features of supernova neutrinos. We do not have the recipe to carry it out. Therefore, we restrict the type of CPT violation to test to the ones signaled by the difference between the masses and the mixing parameters of neutrinos and antineutrinos, assuming that their interactions are described by the standard model.

How can CPT violation be actually signaled by supernova neutrinos? As we will show in the subsequent sections, a possible difference in mass patterns and mixing angles of neutrinos and antineutrinos results in several different spectral patterns of three species of neutrinos, ν_e, $\bar{\nu}_e$, and ν_x, where the last is a collective notation for ν_μ, $\bar{\nu}_\mu$, ν_τ, and $\bar{\nu}_\tau$ (see Sec. III). In this paper, we rely on the assumption that flavor-dependent reconstruction of supernova neutrino fluxes will be done at the time of the next supernova, so that CPT-violating patterns of neutrino spectra can be identified. It may be realized either by arrays of detectors of various types, or by a limited number of them with some ingenious method for analysis. Though highly nontrivial, this type of flavor-dependent reconstruction of supernova neutrino spectra is required anyway to diagnose the core of the supernova in the conventional analysis assuming CPT invariance. The importance of the last point has been emphasized some time ago [18].

Although we formulate the problem of testing CPT with supernova neutrinos in a generic way, we focus on the gross (or ''discrete'') violation of CPT caused by different mass patterns and/or by a possible large difference in the mixing angle θ_{13} in neutrino and antineutrino sectors. Then, we show that the supernova neutrino can be a powerful indicator of CPT violation. Signaling CPT violation can be done by distinguishing spectral patterns of three effective species of neutrinos characteristic to CPT violation, which come from unequal level crossing patterns at the high-density resonance of neutrinos and antineutrinos. It should also be noted that this type of CPT test is quite complementary to the one which measures small differences of neutrino and antineutrino mixing parameters. The method of looking for gross violation of CPT is quite insensitive to the presence of a tiny difference in mixing parameters because the effect we are looking for is robust and depends only upon mass patterns. The issue of the supernova neutrino as a sensitive probe for neutrino mass hierarchy was first discussed in [19].[1]

III. BASIC PROPERTIES OF SUPERNOVA NEUTRINOS AND APPROXIMATIONS INVOLVED IN THE TREATMENT

In this section, we briefly summarize the basic properties of supernova neutrinos and the approximations involved in our treatment. Our description will be a very brief one and we refer to [17] for detailed discussions, on which our treatment and notations will be based. The great simplification that occurred after the work was published is that the large mixing angle (LMA) region of the solar Mikheyev-Smirnov-Wolfenstein solution [24] is selected out both in neutrino and antineutrino sectors by all the solar and the KamLAND experiments, respectively [6,7].

We assume a three-flavor mixing scheme of neutrinos with the standard form [2] of the lepton flavor mixing matrix, the Maki-Nakagawa-Sakata matrix [25],

[1]The paper contains, in addition to the general statement of the utility of supernova neutrinos as a tool of discriminating mass hierarchy, an analysis of SN1987A data which leads the authors to conclude that (in page 306) ''if the temperature ratio $\tau \equiv T_{\nu_x}/T_{\bar{\nu}_e}$ is in the range 1.4–2.0 as the SN simulations indicate, the inverted hierarchy of neutrino masses is disfavored by the neutrino data of SN1987A unless the H resonance is nonadiabatic.'' While it follows the spirit of the earlier analyses [20,21], our analysis using the three-flavor mixing framework has physics consequences quite different from the ones spelled out in these papers. In fact, the ansatz tested in [21] is different from the hypothesis we have tested (which was relatively more disfavored) due to the three-flavor treatment of the problem. We note that most of the criticism posed by Barger *et al.* [22] does *not* apply to our analysis because it does not rely on the goodness of the fit in the likelihood analysis but on the credibility of the parameters obtained as a result of the fit. The nature of this type of analysis was already made fully transparent by Jegerlehner, Neubig, and Raffelt [21] in their thorough analysis done in 1996 [23]. It would be very interesting to come back to the debate after having supernova simulations calibrated by the high-statistics data of future galactic supernova.

$$U = \begin{bmatrix} c_{12}c_{13} & s_{12}c_{13} & s_{13}e^{-i\delta} \\ -s_{12}c_{23} - c_{12}s_{23}s_{13}e^{i\delta} & c_{12}c_{23} - s_{12}s_{23}s_{13}e^{i\delta} & s_{23}c_{13} \\ s_{12}s_{23} - c_{12}c_{23}s_{13}e^{i\delta} & -c_{12}s_{23} - s_{12}c_{23}s_{13}e^{i\delta} & c_{23}c_{13} \end{bmatrix}, \quad (1)$$

where c_{ij} and s_{ij} $(i, j = 1\text{–}3)$ imply $\cos\theta_{ij}$ and $\sin\theta_{ij}$, respectively. The lepton mixing matrix U relates the flavor eigenstate to the mass eigenstate as $\nu_\alpha = U_{\alpha i}\nu_i$, where $\alpha = e, \mu, \tau$ and $i = 1, 2, 3$. The mass squared difference of neutrinos is defined as $\Delta m^2_{ij} \equiv m^2_i - m^2_j$ where m_i is the eigenvalue of the ith mass eigenstate. To distinguish the antineutrino mixing matrix from that of the neutrinos we place a ''bar'' on the corresponding mixing parameters.

In the analysis in this paper, we restrict ourselves to the simplified ansatz for supernova neutrinos. That is, ν_μ, $\bar{\nu}_\mu$, ν_τ, and $\bar{\nu}_\tau$ are treated as a single component denoted as ν_x. It is a good approximation because they interact with surrounding matter only through neutral current interactions, and hence they are practically physically indistinguishable with each other. Under the approximation, supernova neutrinos consist of the three components, ν_e, $\bar{\nu}_e$, and ν_x.

It is in fact very simple to compute the neutrino flux just outside supernova for a given set of neutrino fluxes at a neutrino sphere. To do this one must first draw the level crossing diagrams of neutrinos and antineutrinos, as given in Fig. 1. The characteristic feature of the supernova neutrino level crossing diagram, which is unique among astrophysical objects, is that there are two resonances, one in high and the other low density regions, corresponding, respectively, to the atmospheric and the solar Δm^2 scales. (In a typical supernova progenitor, they are located in helium and hydrogen burning shells, respectively.) They are referred to as the H and the L level crossings in this paper. The level crossing patterns as well as their (non-)adiabaticity are the decisive factors of neutrino flavor conversion in supernova [26].

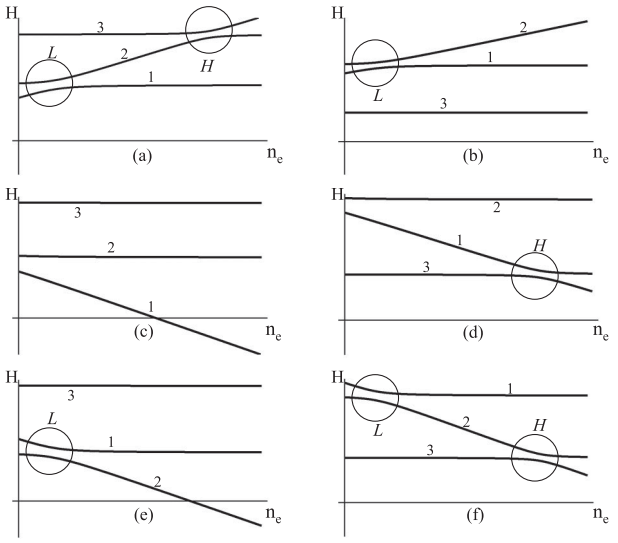

FIG. 1. Level crossing diagrams for neutrino flavor conversion in supernova. In the neutrino sector there are 2 diagrams which correspond to the normal [(a) $\Delta m^2_{31} > 0$] and the inverted [(b) $\Delta m^2_{31} < 0$] hierarchies. In the antineutrino sector there are 4 diagrams which correspond to the normal [(c),(e) $\Delta m^2_{31} > 0$] and the inverted [(d),(f) $\Delta m^2_{31} < 0$] hierarchies, each doubled by two patterns of small mass splittings, the reactor-normal [(c),(d) $\Delta\bar{m}^2_{21} > 0$] the reactor-inverted [(e),(f) $\Delta\bar{m}^2_{21} < 0$] hierarchies. In the CPT invariant case the diagrams (a)– (d) remain.

It should be noticed that, because we are preparing a general CPT noninvariant framework, we have to draw diagrams of ν and $\bar{\nu}$ separately, thereby allowing the cases with different mass hierarchies for neutrinos and antineutrinos. Altogether there are two and four cases of level crossing diagrams, corresponding to the normal and the inverted mass hierarchies in ν and $\bar{\nu}$ sectors, respectively. Proliferation of the $\bar{\nu}$ diagram by a factor of 2 is due to the inability of distinguishing $\bar{m}_2 > \bar{m}_1$ or $\bar{m}_2 < \bar{m}_1$ cases. It should be noticed that one can adopt one of the two conventions, which are equivalent to each other: (1) $\bar{m}_2 > \bar{m}_1$ and $0 < \theta < \pi/2$, or (2) $0 < \theta < \pi/4$ with $\bar{m}_2 > \bar{m}_1$ or $\bar{m}_2 < \bar{m}_1$. In this paper, we take the latter convention.

An enormous simplification results in the treatment of neutrino flavor transformation in supernova (in fact in the envelope of the progenitor star) if the two resonances, H and L, are approximately independent of each other. It was argued in [17] that they are, based on a factor of $\simeq 30$ difference between Δm^2_{31} and Δm^2_{21} but under the assumption that they are identical in neutrino and antineutrino sectors. Fortunately, thanks to the currently available constraints on Δm^2 and $\Delta\bar{m}^2$ which are already rather powerful, we can argue that the same approximation applies even when we relax the assumption that they are identical. We first note that Δm^2_{21} and $\Delta\bar{m}^2{}_{21}$ are both in the ''LMA'' region; they are constrained to be in the regions

$$\begin{aligned} &2 \times 10^{-5}\ \text{eV}^2 \le \Delta m^2_{21} \le 2 \times 10^{-4}\ \text{eV}^2, \\ &10^{-5}\ \text{eV}^2 \le |\Delta\bar{m}^2{}_{21}| \le 2 \times 10^{-4}\ \text{eV}^2, \end{aligned} \quad (2)$$

the former by all the solar neutrino experiments [6], while the latter by the KamLAND experiment [7], both at 3σ C.L. On the other hand, Δm^2_{31} and $\Delta\bar{m}^2{}_{31}$ are constrained to be

$$\begin{aligned} &9 \times 10^{-4}\ \text{eV}^2 \le |\Delta m^2_{31}| \le 6 \times 10^{-3}\ \text{eV}^2, \\ &4.5 \times 10^{-3}\ \text{eV}^2 \le |\Delta\bar{m}^2_{31}| \le 2 \times 10^{-2}\ \text{eV}^2, \end{aligned} \quad (3)$$

at 99% C.L. by the SK atmospheric neutrino data [13]. Because of the factor of about 20 difference it can be argued quite safely that the approximation of independent

H and L resonances applies even in our general setting which accommodates CPT violation.

It may be appropriate to mention here that the currently available bound on possible CPT violation in lepton mixing angles is rather mild, as summarized in [15]. The current bound on the difference between $\sin^2\theta_{12}$ for neutrino and $\sin^2\bar{\theta}_{12}$ for antineutrinos is rather weak [7]. Even if we assume that $\bar{\theta}_{12}$ is in the first octant,

$$|\sin^2\theta_{12} - \sin^2\bar{\theta}_{12}| \leq 0.3, \tag{4}$$

at 99.73% C.L. The bound obtained for θ_{13} is extremely weak; $|\sin^2\theta_{13} - \sin^2\bar{\theta}_{13}|$ can be almost unity [12].

IV. CLASSIFICATION OF PATTERNS OF SUPERNOVA NEUTRINO SPECTRA

In this section, after recollecting compact formulas for neutrino flavor conversion in supernova (Sec. IV A), we present a complete classification of spectral patterns of supernova neutrinos (Sec. IV B). The cases of reduced degeneracy by the aid of additional information from accelerator and reactor experiments will be discussed in Sec. V. The general characteristics of the different flux patterns will be described in Sec. VI. We will discuss in Sec. VII to what extent this additional information helps to discriminate flux patterns by limiting the number of possibilities.

A. Neutrino and antineutrino spectra with LMA solution

Under the approximations spelled out in the previous section, the neutrino fluxes that are to reach terrestrial detectors can be written in the compact notation [17]

$$\begin{pmatrix} F_e \\ F_{\bar{e}} \\ 4F_x \end{pmatrix} = \begin{pmatrix} p & 0 & 1-p \\ 0 & \bar{p} & 1-\bar{p} \\ 1-p & 1-\bar{p} & 2+p+\bar{p} \end{pmatrix} \begin{pmatrix} F_e^0 \\ F_{\bar{e}}^0 \\ F_x^0 \end{pmatrix}. \tag{5}$$

The above general expression holds for both the normal and the inverted mass hierarchies. By "normal" and "inverted" we mean $\Delta m^2_{31} > 0$ and $\Delta m^2_{31} < 0$, which will be denoted hereafter with subscripts N and I, respectively, Though it is known that $\Delta m^2_{21} > 0$ by the solar neutrino observation, there are two possible subclasses in the antineutrino sector: $\Delta\bar{m}^2_{21} > 0$ and $\Delta\bar{m}^2_{21} < 0$ as noted in [27]. The former and the latter will be referred to as the reactor-normal and the reactor-inverted hierarchies, respectively. We will keep this distinction with the use of the combined subscripts as $N21$ and $I21$ ($N12$ and $I12$) for $\Delta\bar{m}^2_{21} > 0$ ($\Delta\bar{m}^2_{21} < 0$) in the case of normal and inverted hierarchies, respectively. Altogether there are two and four different level crossing patterns in neutrino and antineutrino sectors, respectively. They are depicted in Fig. 1.

The ν_e and $\bar{\nu}_e$ survival probabilities p and $\bar{p}$'s are given with the use of the jumping probabilities P_H and P_L at H and L level crossings as

$$p_N = |U_{e1}|^2 P_H P_L + |U_{e2}|^2 P_H (1-P_L) + |U_{e3}|^2 (1-P_H), \tag{6}$$

$$\bar{p}_{N21} = |\bar{U}_{e1}|^2, \tag{7}$$

$$\bar{p}_{N12} = |\bar{U}_{e1}|^2 \bar{P}_L + |\bar{U}_{e2}|^2 (1-\bar{P}_L), \tag{8}$$

for the normal hierarchy and

$$p_I = |U_{e1}|^2 P_L + |U_{e2}|^2 (1-P_L), \tag{9}$$

$$\bar{p}_{I21} = |\bar{U}_{e1}|^2 \bar{P}_H + |\bar{U}_{e3}|^2 (1-\bar{P}_H), \tag{10}$$

$$\bar{p}_{I12} = |\bar{U}_{e1}|^2 \bar{P}_H \bar{P}_L + |\bar{U}_{e2}|^2 \bar{P}_H (1-\bar{P}_L) + |\bar{U}_{e3}|^2 (1-\bar{P}_H), \tag{11}$$

for the inverted hierarchy.

We note that Δm^2_{21} and $\Delta\bar{m}^2{}_{21}$ are both in the LMA region; the former is constrained to be in the region $2 \times 10^{-5}\ \mathrm{eV}^2 < \Delta m^2_{21} < 2 \times 10^{-4}\ \mathrm{eV}^2$ by all the solar neutrino experiments while the latter is $10^{-5}\ \mathrm{eV}^2 < \Delta\bar{m}^2{}_{21} < 2 \times 10^{-4}\ \mathrm{eV}^2$ by the KamLAND experiments, both at the 3σ C.L. Then, one can argue quite safely that the L level crossings are adiabatic not only in the neutrino but also in the antineutrino channels, $P_L = \bar{P}_L = 0$. Then, the survival factors take simple forms

$$p_N = |U_{e2}|^2 P_H + |U_{e3}|^2 (1-P_H), \tag{12}$$

$$\bar{p}_{N21} = |\bar{U}_{e1}|^2, \tag{13}$$

$$\bar{p}_{N12} = |\bar{U}_{e2}|^2, \tag{14}$$

for the normal hierarchy and

$$p_I = |U_{e2}|^2, \tag{15}$$

$$\bar{p}_{I21} = |\bar{U}_{e1}|^2 \bar{P}_H + |\bar{U}_{e3}|^2 (1-\bar{P}_H), \tag{16}$$

$$\bar{p}_{I12} = |\bar{U}_{e2}|^2 \bar{P}_H + |\bar{U}_{e3}|^2 (1-\bar{P}_H), \tag{17}$$

for the inverted hierarchy. Therefore, the distinction between $\Delta\bar{m}^2_{21} > 0$ and $\Delta\bar{m}^2_{21} < 0$ cases is just interchanging $|\bar{U}_{e1}|$ and $|\bar{U}_{e2}|$, as expected.

We make a short remark on possible roles played by the earth matter effect [17]. It is well known that if the H resonance is adiabatic it plays no role. In the case of nonadiabatic H resonance, it can play a role but again it is suppressed by the factor $(2Ea_{\mathrm{earth}}/\Delta m^2_{31})\sin^2 2\theta_{13}$, where $a = \sqrt{2}G_F N_e(x)$ is related to the neutrino's index of refraction in matter with G_F and N_e being the Fermi constant and the electron number density, respectively. An explicit computation reveals that the effects of the earth matter effect is small, and moreover it cannot lift the degeneracy between the CPT-conserving and CPT-violating cases. Therefore, we do not discuss it further in the present paper.

B. General classification of patterns of supernova neutrino spectra

In the rest of this paper, we focus on the cases in which the H level crossing is completely adiabatic or nonadiabatic; we do not discuss the intermediate case in which the H level crossing is an admixture of adiabatic and nonadiabatic transitions. By doing so we restrict ourselves to the two regions of θ_{13}, roughly speaking, $s^2_{13} \geq 10^{-4}$ (adiabatic), or $s^2_{13} \leq 10^{-6}$ (nonadiabatic). We can classify the possible situation into $4 \times 8 = 32$ cases depending upon the following: (i) neutrino and antineutrino mass patterns are either normal or inverted, and if $\Delta\bar{m}^2_{21} > 0$ or $\Delta\bar{m}^2_{21} < 0$ in the antineutrino sector, (ii) the H level crossings in neutrino and antineutrino sectors are adiabatic or nonadiabatic, as given in Table I. In each case, the neutrino fluxes F_e, $F_{\bar{e}}$, and F_x at a detector can be predicted for a given set of F^0_e, $F^0_{\bar{e}}$, and F^0_x at a neutrino sphere.

From the viewpoint of neutrino flavor transformation, however, there are enormous degeneracies in the 32 cases. First of all, the duplication due to the adiabatic and nonadiabatic H level crossing in the columns of p_I, $\bar{p}_{N21}$, and $\bar{p}_{N12}$ [Figs. 1(*b*), (*c*), (*e*)] are superficial because of no H level crossing. In fact, one can show from Table I that there are only 6 different patterns of the neutrino spectra:

$$
\begin{aligned}
&P_{31}\text{: } p = |U_{e3}|^2,\ \bar{p} = |\bar{U}_{e1}|^2,\\
&P_{23}\text{: } p = |U_{e2}|^2,\ \bar{p} = |\bar{U}_{e3}|^2,\\
&P_{21}\text{: } p = |U_{e2}|^2,\ \bar{p} = |\bar{U}_{e1}|^2,\\
&P_{32}\text{: } p = |U_{e3}|^2,\ \bar{p} = |\bar{U}_{e2}|^2,\\
&P_{33}\text{: } p = |U_{e3}|^2,\ \bar{p} = |\bar{U}_{e3}|^2,\\
&P_{22}\text{: } p = |U_{e2}|^2,\ \bar{p} = |\bar{U}_{e2}|^2.
\end{aligned}
\tag{18}
$$

Each pattern contains several cases of ν and $\bar{\nu}$ mass hierarchies and (non-)adiabaticity of H resonance. Notice, however, that all the 32 cases must be treated as different scenarios from a particle physics point of view. Despite degeneracies in the features of flavor conversion, each of the degenerate scenarios sometimes has different CPT transformation properties.

We use abbreviated notation to represent them. For example, (ν: N-AD, $\bar{\nu}$: I-NAD) implies that neutrinos have the normal mass hierarchy and the adiabatic H level crossing, and antineutrinos have the inverted mass hierarchy and the nonadiabatic H level crossing. Then, the content of each flux pattern is

P_{31}: (ν: N-AD, $\bar{\nu}$: $N21$-AD), <u>(ν: N-AD, $\bar{\nu}$: $N21$-NAD)</u>, <u>(ν: N-AD, $\bar{\nu}$: $I21$-NAD)</u>,

P_{23}: <u>(ν: N-NAD, $\bar{\nu}$: $I21$-AD)</u>, <u>(ν: N-NAD, $\bar{\nu}$: $I12$-AD)</u>, (ν: I-AD, $\bar{\nu}$: $I21$-AD),
<u>(ν: I-AD, $\bar{\nu}$: $I12$-AD)</u>, <u>(ν: I-NAD, $\bar{\nu}$: $I21$-AD)</u>, <u>(ν: I-NAD, $\bar{\nu}$: $I12$-AD)</u>,

P_{21}: <u>(ν: N-NAD, $\bar{\nu}$: $N21$-AD)</u>, (ν: N-NAD, $\bar{\nu}$: $N21$-NAD), <u>(ν: N-NAD, $\bar{\nu}$: $I21$-NAD)</u>,
<u>(ν: I-AD, $\bar{\nu}$: $N21$-AD)</u>, <u>(ν: I-AD, $\bar{\nu}$: $N21$-NAD)</u>, <u>(ν: I-AD, $\bar{\nu}$: $I21$-NAD)</u>, <u>(ν: I-NAD, $\bar{\nu}$: $N21$-AD)</u>,
<u>(ν: I-NAD, $\bar{\nu}$: $N21$-NAD)</u>, (ν: I-NAD, $\bar{\nu}$: $I21$-NAD), (19)

P_{32}: <u>(ν: N-AD, $\bar{\nu}$: $N12$-AD)</u>, <u>(ν: N-AD, $\bar{\nu}$: $N12$-NAD)</u>, <u>(ν: N-AD, $\bar{\nu}$: $I12$-NAD)</u>,

P_{33}: <u>(ν: N-AD, $\bar{\nu}$: $I21$-AD)</u>, <u>(ν: N-AD, $\bar{\nu}$: $I12$-AD)</u>,

P_{22}: <u>(ν: N-NAD, $\bar{\nu}$: $N12$-AD)</u>, <u>(ν: N-NAD, $\bar{\nu}$: $N12$-NAD)</u>, <u>(ν: N-NAD, $\bar{\nu}$: $I12$-NAD)</u>, <u>(ν: I-AD, $\bar{\nu}$: $N12$-AD)</u>,
<u>(ν: I-AD, $\bar{\nu}$: $N12$-NAD)</u>, <u>(ν: I-AD, $\bar{\nu}$: $I12$-NAD)</u>, <u>(ν: I-NAD, $\bar{\nu}$: $N12$-AD)</u>, <u>(ν: I-NAD, $\bar{\nu}$: $N12$-NAD)</u>,
<u>(ν: I-NAD, $\bar{\nu}$: $I12$-NAD)</u>,

where the one with (without) the underline indicates the case with (without) CPT violation. Several immediate comments are in order: Most notably, only the CPT-violating cases are involved in the latter three patterns P_{32}, P_{33}, and P_{22}. Whereas

TABLE I. The electron neutrino and antineutrino survival factors p and $\bar{p}$ are presented for adiabatic and nonadiabatic H level crossings. Note that the apparent duplication due to the adiabatic and nonadiabatic H level crossings in the columns of p_I, $\bar{p}_{N21}$, and $\bar{p}_{N12}$ is superficial for flavor conversion in supernova because of no H level crossing.

$\nu/\bar{\nu}$ survival factor adiabaticity	p_N	p_I	$\bar{p}_{N21}$	$\bar{p}_{N12}$	$\bar{p}_{I21}$	$\bar{p}_{I12}$
Adiabatic H crossing	$\lvert U_{e3}\rvert^2$	$\lvert U_{e2}\rvert^2$	$\lvert \bar{U}_{e1}\rvert^2$	$\lvert \bar{U}_{e2}\rvert^2$	$\lvert \bar{U}_{e3}\rvert^2$	$\lvert \bar{U}_{e3}\rvert^2$
Nonadiabatic H crossing	$\lvert U_{e2}\rvert^2$	$\lvert U_{e2}\rvert^2$	$\lvert \bar{U}_{e1}\rvert^2$	$\lvert \bar{U}_{e2}\rvert^2$	$\lvert \bar{U}_{e1}\rvert^2$	$\lvert \bar{U}_{e2}\rvert^2$

the first three patterns P_{31}, P_{23}, and P_{21} contain CPT-conserving as well as violating cases; there are only 4 CPT-conserving cases, two in P_{21}, and one in each of P_{23} and in P_{31}, and the remaining 28 cases are CPT violating.

Therefore, if one is able to disentangle the latter three patterns observationally, the future supernova neutrino detection has a potential to discover CPT violation. We will discuss this possibility further in the subsequent sections. In the rest of the patterns P_{21}, P_{23}, and P_{31}, with the coexistence of CPT-violating and CPT-conserving cases, the observation of supernova neutrinos by itself cannot signal CPT violation nor prove CPT invariance. However, there are possibilities that one can make stronger cases with the help of terrestrial experiments as we discuss in the next section.

V. CASE OF REDUCED DEGENERACY WITH HELP OF OTHER TYPES OF EXPERIMENTS

There are several cases in which CPT violation can be signaled more easily by combining supernova ν and $\bar{\nu}$ observations with some other experiments. It occurs, in particular, in the case where the next generation accelerator [28–31] and/or the reactor experiments [32] are able to measure θ_{13}, or go down to the sensitivity to establish a nonadiabatic H level crossing [33]. At this stage, it may be possible that some experiments can determine the neutrino mass hierarchy. For recent discussions, see e.g., [34]. We explore in this section what would be the effect of these additional inputs for uncovering CPT violation. We do not discuss the cases in which CPT violation is already obvious by this additional information, for example, the cases such as normal neutrino and inverted antineutrino mass hierarchies, or how the measured values of θ_{ij} and $\bar{\theta}_{ij}$ differ with each other at a high confidence level.

A. Detection of θ_{13} in reactor and accelerator experiments

If the next generation accelerator experiments and/or the reactor measurement succeed to detect the effect of nonvanishing θ_{13} and $\bar{\theta}_{13}$, respectively, it means that $P_H = \bar{P}_H = 0$. Then, the degeneracy shrinks enormously. In each pattern of masses and level crossings, the cases which remain are

$$\begin{aligned}
&P_{31}\text{: } (\nu\text{: } N\text{-AD, } \bar{\nu}\text{: } N21\text{-AD}),\\
&P_{23}\text{: } (\nu\text{: } I\text{-AD, } \bar{\nu}\text{: } I21\text{-AD}), \underline{(\nu\text{: } I\text{-AD, } \bar{\nu}\text{: } I12\text{-AD})},\\
&P_{21}\text{: } \underline{(\nu\text{: } I\text{-AD, } \bar{\nu}\text{: } N21\text{-AD})},\\
&P_{32}\text{: } \underline{(\nu\text{: } N\text{-AD, } \bar{\nu}\text{: } N12\text{-AD})},\\
&P_{33}\text{: } \underline{(\nu\text{: } N\text{-AD, } \bar{\nu}\text{: } I21\text{-AD})}, \underline{(\nu\text{: } N\text{-AD, } \bar{\nu}\text{: } I12\text{-AD})},\\
&P_{22}\text{: } \underline{(\nu\text{: } I\text{-AD, } \bar{\nu}\text{: } N12\text{-AD})}.
\end{aligned} \tag{20}$$

A novel feature of (20) is that the patterns P_{21} and P_{31} now contain only the CPT-violating and CPT-conserving cases, respectively. In this case it is sufficient to exclude the patterns P_{23} and P_{31} to establish CPT violation.

B. No signal of θ_{13} in future terrestrial experiments

Suppose that, instead of positive detection which was assumed in the above, no indication for nonzero θ_{13} and $\bar{\theta}_{13}$ is obtained by the next generation accelerator and reactor experiments. If it continues to be true to the extreme sensitivity reachable by a neutrino factory, it would imply that $P_H = \bar{P}_H = 1$. Then, the degeneracy again decreases enormously, but in a quite different way of adiabatic H resonances,

$$\begin{aligned}
&P_{21}\text{: } (\nu\text{: } N\text{-NAD, } \bar{\nu}\text{: } N21\text{-NAD}), \underline{(\nu\text{: } N\text{-NAD, } \bar{\nu}\text{: } I21\text{-NAD})},\\
&\quad \underline{(\nu\text{: } I\text{-NAD, } \bar{\nu}\text{: } N21\text{-NAD})}, (\nu\text{: } I\text{-NAD, } \bar{\nu}\text{: } I21\text{-NAD}),\\
&P_{22}\text{: } \underline{(\nu\text{: } N\text{-NAD, } \bar{\nu}\text{: } N12\text{-NAD})}, \underline{(\nu\text{: } N\text{-NAD, } \bar{\nu}\text{: } I12\text{-NAD})},\\
&\quad \underline{(\nu\text{: } I\text{-NAD, } \bar{\nu}\text{: } N12\text{-NAD})}, \underline{(\nu\text{: } I\text{-NAD, } \bar{\nu}\text{: } I12\text{-NAD})},\\
&P_{23}, P_{31}, P_{32}, P_{33}\text{: no case remains.}
\end{aligned} \tag{21}$$

Only two patterns, P_{21} and P_{22}, are allowed. The rejection of P_{21} or the confirmation of P_{22} implies CPT violation.

C. The normal ν and $\bar{\nu}$ mass hierarchies

If the neutrino and antineutrino mass hierarchies are both normal ($\Delta m^2_{31} > 0$) and if the value of θ_{13} is not known, only four flux patterns remain:

$$\begin{aligned}
&P_{31}\text{: } (\nu\text{: } N\text{-AD, } \bar{\nu}\text{: } N21\text{-AD}), \underline{(\nu\text{: } N\text{-AD, } \bar{\nu}\text{: } N21\text{-NAD})},\\
&P_{21}\text{: } \underline{(\nu\text{: } N\text{-NAD, } \bar{\nu}\text{: } N21\text{-AD})}, (\nu\text{: } N\text{-NAD, } \bar{\nu}\text{: } N21\text{-NAD}),\\
&P_{32}\text{: } \underline{(\nu\text{: } N\text{-AD, } \bar{\nu}\text{: } N12\text{-AD})}, \underline{(\nu\text{: } N\text{-AD, } \bar{\nu}\text{: } N12\text{-NAD})},\\
&P_{22}\text{: } \underline{(\nu\text{: } N\text{-NAD, } \bar{\nu}\text{: } N12\text{-AD})}, \underline{(\nu\text{: } N\text{-NAD, } \bar{\nu}\text{: } N12\text{-NAD})}.
\end{aligned} \tag{22}$$

Rejection of the flux patterns P_{31} and P_{21} or confirmation of the patterns P_{32} and P_{22} establishes CPT violation.[2]

D. The inverted ν and $\bar{\nu}$ mass hierarchies

If the neutrino and antineutrino mass hierarchies are both the inverted type ($\Delta m^2_{31} < 0$) and if the value of θ_{13} is not known, only three flux patterns remain:

$$\begin{aligned}
&P_{23}\text{: } (\nu\text{: } I\text{-AD, } \bar{\nu}\text{: } I21\text{-AD}), \underline{(\nu\text{: } I\text{-AD, } \bar{\nu}\text{: } I12\text{-AD})},\\
&\quad \underline{(\nu\text{: } I\text{-NAD, } \bar{\nu}\text{: } I21\text{-AD})}, \underline{(\nu\text{: } I\text{-NAD, } \bar{\nu}\text{: } I12\text{-AD})},\\
&P_{21}\text{: } \underline{(\nu\text{: } I\text{-AD, } \bar{\nu}\text{: } I21\text{-NAD})}, (\nu\text{: } I\text{-NAD, } \bar{\nu}\text{: } I21\text{-NAD}),\\
&P_{22}\text{: } \underline{(\nu\text{: } I\text{-AD, } \bar{\nu}\text{: } I12\text{-NAD})}, \underline{(\nu\text{: } I\text{-NAD, } \bar{\nu}\text{: } I12\text{-NAD})}.
\end{aligned} \tag{23}$$

[2]Notice that the logic here is even if the sign of Δm^2_{31} is measured only for neutrinos, for example, we assume the same sign for antineutrinos and yet the analysis can signal CPT violation.

To single out the pattern P_{22} appears to be the easiest way to demonstrate CPT violation.

Under the assumptions made in Secs. V B, V C, and V D, CPT violation, once demonstrated, implies the reactor-inverted antineutrino mass hierarchy, $\bar{m}_2 < \bar{m}_1$. Or, equivalently, $\bar{\theta}_{12}$ is in the dark side. Thus, supernova neutrinos can in principle have sensitivity to the $\bar{\theta}_{12}$ light-side vs dark-side confusion. Below, we examine the cases of additional inputs combined.

E. Adiabatic H resonance and the normal or the inverted mass hierarchies

If the H resonance is adiabatic, and if the neutrino and antineutrino mass hierarchies are both normal only two flux patterns remain:

$$\begin{aligned} &P_{31}\text{: } (\nu\text{: } N\text{-AD, } \bar{\nu}\text{: } N21\text{-AD}), \\ &P_{32}\text{: } \underline{(\nu\text{: } N\text{-AD, } \bar{\nu}\text{: } N12\text{-AD}).} \end{aligned} \tag{24}$$

If the H resonance is adiabatic, and if the neutrino and antineutrino mass hierarchies are both inverted the allowed flux pattern is unique:

$$P_{23}\text{: } (\nu\text{: } I\text{-AD, } \bar{\nu}\text{: } I21\text{-AD}), \underline{(\nu\text{: } I\text{-AD, } \bar{\nu}\text{: } I12\text{-AD}).} \tag{25}$$

In this case, there is no way of telling whether CPT is violated or not in our method.

F. Nonadiabatic H resonance and the normal or the inverted mass hierarchies

If the H resonance is nonadiabatic, a distinction between mass hierarchies, normal vs inverted, does not make difference in the allowed flux patterns:

$$\begin{aligned} &P_{21}\text{: } (\nu\text{: } X\text{-NAD, } \bar{\nu}\text{: } X21\text{-NAD}), \\ &P_{22}\text{: } \underline{(\nu\text{: } X\text{-NAD, } \bar{\nu}\text{: } X12\text{-NAD}),} \end{aligned} \tag{26}$$

where X can be N (normal) or I (inverted). Note that the two flux patterns are different from (24).

VI. CHARACTERISTIC FEATURES OF PATTERN DEPENDENT NEUTRINO FLUXES

We now discuss the characteristic features of neutrino spectra of e, $\bar{e}$, and x flavors in each classified pattern of neutrino flavor transformation in supernova. So far we have formulated, in a generic way, the method for testing CPT violation with supernova neutrinos. In the rest of this paper, we concentrate on testing CPT violation caused by the difference between neutrino and antineutrino mass patterns as well as their mixing angles θ_{13} and $\bar{\theta}_{13}$. We take $\theta_{12} = \bar{\theta}_{12}$ in the following analysis. (Note that all the mixing angles are in the first octant in our convention, and θ_{23} does not come into play.) In some cases based on the Garching simulation we need enormous accuracies of less than a few % to distinguish between various spectral patterns (see Sec. VII). In such cases there is no hope of establishing CPT violation if the effects caused by small differences in the mixing angle θ_{12} in ν and $\bar{\nu}$ sectors and the one from the neutrino mass pattern coexist.

Though the current bounds on the difference between θ_{12} and $\bar{\theta}_{12}$ are rather mild ones it is quite possible that the room between them will tighten up as the KamLAND experiment proceeds. The choice $\theta_{12} = \bar{\theta}_{12}$ could become mandatory if the low-energy solar neutrino measurement [35] and the dedicated reactor $\bar{\theta}_{12}$ experiments [15,36] are both realized.

A. Characteristic features of spectral patterns of neutrino fluxes

To give the readers a feeling if the neutrino spectra that arise in the six different patterns can be distinguished, we give an illustration using a model flux based on the Livermore simulation [37]. The parameters that characterize the spectral form of the flux are given in Table III in Sec. VII, where a comparison between the results with the other two flux models based on the Garching simulation is carried out. In this subsection we employ the Livermore flux because it is, at least, most suitable for illustrative purposes, having clear differences among spectral shapes of three effective neutrino species, as shown in Fig. 2. We note that the results with the Livermore parameters are very similar to the ones with the pinched Fermi-Dirac distribution used in a vast amount of literatures, e.g., in [17,38].

We draw in Fig. 3 the spectra of the three effective neutrino species ν_e, $\bar{\nu}_e$, and ν_x of six different patterns of P_{31} to P_{22} defined in (18). One can recognize that the six patterns of neutrino flavor conversion in supernova are quite different from each other partly due to the ''optimistic'' choice of the parameters. The difference in the spectral patterns in three species of neutrinos is the key to discriminate six different scenarios of flavor transforma-

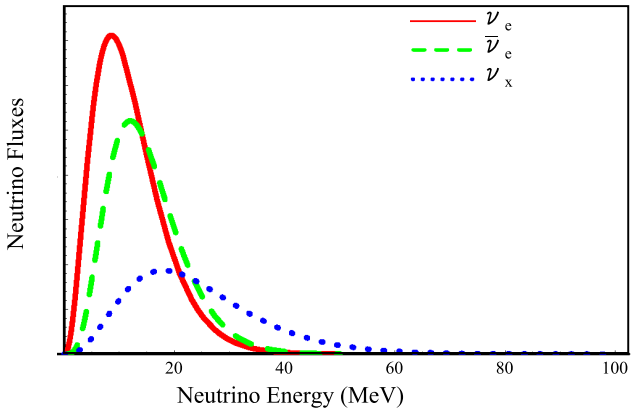

FIG. 2 (color online). The primary energy spectra of three effective neutrino species ν_e (red solid curve), $\bar{\nu}_e$ (green dashed curve), and ν_x (blue dotted curve) of neutrinos just outside the neutrino sphere are shown. The flux model is based on the Livermore simulation whose parameters are given in Table III in Sec. VII. The absolute normalization is arbitrary.

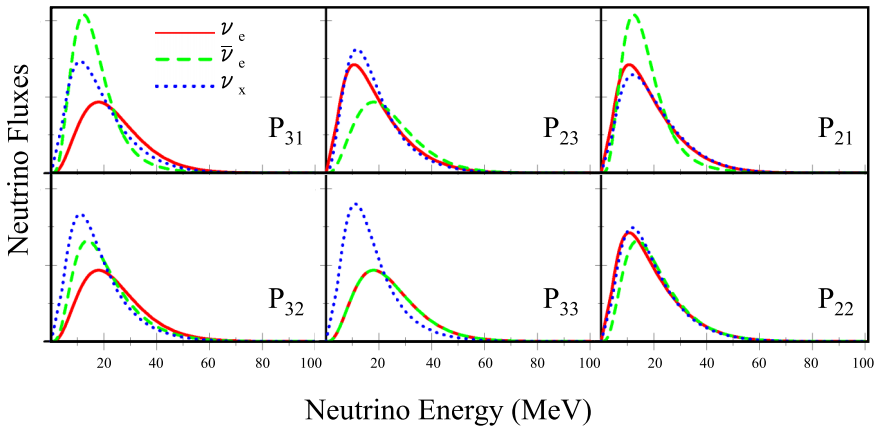

FIG. 3 (color online). The energy spectra of the three effective neutrino species ν_e (red solid curves), $\bar{\nu}_e$ (green dashed curves), and ν_x (blue dotted curves) at terrestrial detectors corresponding to six different patterns of neutrino flavor conversion P_{31} to P_{22} defined in (18) are presented. The Livermore flux model with the same values of parameters as in Fig. 2 is used. Although an overall absolute normalization is arbitrary, the relative normalization between the six patterns is meaningful.

tion. For more quantitative understanding, we give in Table II the average values of energies $\langle E_\alpha \rangle$ ($\alpha = e$, $\bar{e}$ and x), and the width parameter $\langle \Delta E_\alpha \rangle \equiv \sqrt{\langle E_\alpha^2 \rangle - \langle E_\alpha \rangle^2}$ which is also used in [40]. To make the distinction among the six patterns clearer we also give in Table II the ratios $\langle E_\beta \rangle / \langle E_{\bar{e}} \rangle$ and $\langle \Delta E_\beta \rangle / \langle \Delta E_{\bar{e}} \rangle$ for $\beta = e$ and x, assuming that the denominators would be the best determined parameters. The distinction between the different flavor conversion patterns is obvious.

Notice that the upper three patterns, P_{31}, P_{23}, and P_{21} contain CPT-conserving as well as violating cases, whereas the lower three patterns P_{32}, P_{33}, and P_{22} consist solely of CPT-violating ones. Therefore, the above discussion applies, upon restriction to the upper three cases, to the conventional CPT-conserving cases as well.

We make comments on some notable features of the results presented in Table II.

(i) *CPT-conserving cases.*—It may be instructive to understand the feature of the CPT-conserving cases contained in the patterns P_{31}, P_{23}, and P_{21}. In the pattern P_{31} (the case of normal hierarchy and adiabatic H resonance) the H resonance is in the neutrino channel, and $\langle E_e \rangle / \langle E_{\bar{e}} \rangle > 1$ because ν_e at the terrestrial detector is dominantly composed of ν_x at the neutrinosphere [26]. In the pattern P_{23} (the case of inverted hierarchy and adiabatic H resonance) the H resonance is in the antineutrino channel, and therefore $\langle E_e \rangle / \langle E_{\bar{e}} \rangle < 1$. The distinction between P_{31} and P_{23} allows one to distinguish the normal and the inverted mass hierarchies [19]. In the pattern P_{21} (the case of nonadiabatic H resonance) ν_e ($\bar{\nu}_e$) at the earth are superpositions of ν_e ($\bar{\nu}_e$) and ν_x at the neutrinosphere. These features are extensively discussed by many authors [17,19,38,40–44].

(ii) *CPT-violating cases.*—As one can recognize from Table II there is a general tendency that $\langle E_x \rangle / \langle E_{\bar{e}} \rangle$ is small in CPT-violating cases. Unfortunately, it does not guarantee unique identification of them because of the similar small ratio of P_{23}. But the latter has a distinctive feature that all the ratios $\langle E_\alpha \rangle / \langle E_{\bar{e}} \rangle$ and $\langle \Delta E_\alpha \rangle / \langle \Delta E_{\bar{e}} \rangle$ ($\alpha = e, x$) are smaller than unity. The feature may allow unique identifi-

TABLE II. The averaged energies and the width parameters of three species of neutrinos are presented by using the spectra based on the Livermore simulation with the parameters given in Table III. The upper three patterns, P_{31}, P_{23}, and P_{21} contain CPT-conserving as well as violating cases, whereas the lower three patterns P_{32}, P_{33}, and P_{22} consist solely of CPT-violating ones.

Spectral patterns	$\langle E_e \rangle$	$\langle E_{\bar{e}} \rangle$	$\langle E_x \rangle$	$\langle \Delta E_e \rangle$	$\langle \Delta E_{\bar{e}} \rangle$	$\langle \Delta E_x \rangle$	$\frac{\langle E_e \rangle}{\langle E_{\bar{e}} \rangle}$	$\frac{\langle E_x \rangle}{\langle E_{\bar{e}} \rangle}$	$\frac{\langle \Delta E_e \rangle}{\langle \Delta E_{\bar{e}} \rangle}$	$\frac{\langle \Delta E_x \rangle}{\langle \Delta E_{\bar{e}} \rangle}$
P_{31}	24.0	16.8	18.6	12.0	8.8	11.3	1.43	1.10	1.36	1.29
P_{23}	18.7	24.0	18.1	11.6	12.0	10.7	0.78	0.75	0.96	0.89
P_{21}	18.7	16.8	19.6	11.6	8.8	11.6	1.11	1.17	1.31	1.32
P_{32}	24.0	20.5	17.7	12.0	11.1	10.7	1.17	0.86	1.07	0.96
P_{33}	24.0	24.0	17.1	12.0	12.0	10.3	1.0	0.71	1.0	0.86
P_{22}	18.7	20.5	17.7	11.6	11.2	12.6	0.91	0.86	1.04	1.13

cation of P_{23}, and hence that of CPT-violating cases by elimination.

B. Approximate analytic expression of the flux composition

To facilitate a clear understanding and to complement the drawing of figures we give approximate expressions of fluxes. They will help in understanding the features of Fig. 3. We use the approximations $s_{13} \ll 1$ and $\bar{s}_{13} \ll 1$ (assuming that the former is true) which are numerically valid. Notice that it *does not* mean that we restrict ourselves to the case of a nonadiabatic H-level crossing. The approximation applies to the expressions of fluxes after taking $P_H = 0$ or $P_H = 1$ etc. to merely simplify the expressions.

(i) *Pattern* P_{31}.—In this case $p = |U_{e3}|^2 = s_{13}^2$ and $\bar{p} = |\bar{U}_{e1}|^2 = \bar{c}_{12}^2\bar{c}_{13}^2$. Then, the ν_e, $\bar{\nu}_e$, and ν_x spectra are given by

$$\begin{aligned} F_e &= s_{13}^2 F_e^0 + c_{13}^2 F_x^0 \approx F_x^0, \\ F_{\bar{e}} &= \bar{c}_{12}^2\bar{c}_{13}^2 F_{\bar{e}}^0 + (1 - \bar{c}_{12}^2\bar{c}_{13}^2)F_x^0 \\ &\approx \bar{c}_{12}^2 F_{\bar{e}}^0 + \bar{s}_{12}^2 F_x^0, \\ 4F_x &= c_{13}^2 F_e^0 + (1 - \bar{c}_{12}^2\bar{c}_{13}^2)F_{\bar{e}}^0 \\ &\quad + (2 + s_{13}^2 + \bar{c}_{12}^2\bar{c}_{13}^2)F_x^0 \\ &\approx F_e^0 + \bar{s}_{12}^2 F_{\bar{e}}^0 + (2 + \bar{c}_{12}^2)F_x^0. \end{aligned} \tag{27}$$

(ii) *Pattern* P_{23}.—In this case $p = |U_{e2}|^2 = s_{12}^2 c_{13}^2$ and $\bar{p} = |\bar{U}_{e3}|^2 = \bar{s}_{13}^2$. Then, the ν_e, $\bar{\nu}_e$, and ν_x spectra are given by

$$\begin{aligned} F_e &= s_{12}^2 c_{13}^2 F_e^0 + (1 - s_{12}^2 c_{13}^2)F_x^0 \\ &\approx s_{12}^2 F_e^0 + c_{12}^2 F_x^0, \\ F_{\bar{e}} &= \bar{s}_{13}^2 F_e^0 + \bar{c}_{13}^2 F_x^0 \approx F_x^0, \\ 4F_x &= (1 - s_{12}^2 c_{13}^2)F_e^0 + \bar{c}_{13}^2 F_{\bar{e}}^0 \\ &\quad + (2 + s_{12}^2 c_{13}^2 + \bar{s}_{13}^2)F_x^0 \\ &\approx c_{12}^2 F_e^0 + F_{\bar{e}}^0 + (2 + s_{12}^2)F_x^0. \end{aligned} \tag{28}$$

(iii) *Pattern* P_{21}.—In this case $p = |U_{e2}|^2 = s_{12}^2 c_{13}^2$ and $\bar{p} = |\bar{U}_{e1}|^2 = \bar{c}_{12}^2\bar{c}_{13}^2$. Then, the ν_e, $\bar{\nu}_e$, and ν_x spectra are given by

$$\begin{aligned} F_e &= s_{12}^2 c_{13}^2 F_e^0 + (1 - s_{12}^2 c_{13}^2)F_x^0 \\ &\approx s_{12}^2 F_e^0 + c_{12}^2 F_x^0, \\ F_{\bar{e}} &= \bar{c}_{12}^2\bar{c}_{13}^2 F_{\bar{e}}^0 + (1 - \bar{c}_{12}^2\bar{c}_{13}^2)F_x^0 \\ &\approx \bar{c}_{12}^2 F_{\bar{e}}^0 + \bar{s}_{12}^2 F_x^0, \\ 4F_x &= (1 - s_{12}^2 c_{13}^2)F_e^0 + (1 - \bar{c}_{12}^2\bar{c}_{13}^2)F_{\bar{e}}^0 \\ &\quad + (2 + s_{12}^2 c_{13}^2 + \bar{c}_{12}^2\bar{c}_{13}^2)F_x^0 \\ &\approx c_{12}^2 F_e^0 + \bar{s}_{12}^2 F_{\bar{e}}^0 + (2 + s_{12}^2 + \bar{c}_{12}^2)F_x^0. \end{aligned} \tag{29}$$

(iv) *Pattern* P_{32}.—This case contains only CPT-violating patterns. In this case $p = |U_{e3}|^2 = s_{13}^2$ and $\bar{p} = |\bar{U}_{e2}|^2 = \bar{s}_{12}^2\bar{c}_{13}^2$. Then, the ν_e, $\bar{\nu}_e$, and ν_x spectra are given by

$$\begin{aligned} F_e &= s_{13}^2 F_e^0 + c_{13}^2 F_x^0 \approx F_x^0, \\ F_{\bar{e}} &= \bar{s}_{12}^2\bar{c}_{13}^2 F_{\bar{e}}^0 + (1 - \bar{s}_{12}^2\bar{c}_{13}^2)F_x^0 \\ &\approx \bar{s}_{12}^2 F_{\bar{e}}^0 + \bar{c}_{12}^2 F_x^0, \\ 4F_x &= c_{13}^2 F_e^0 + (1 - \bar{s}_{12}^2\bar{c}_{13}^2)F_{\bar{e}}^0 \\ &\quad + (2 + s_{13}^2 + \bar{s}_{12}^2\bar{c}_{13}^2)F_x^0 \\ &\approx F_e^0 + \bar{c}_{12}^2 F_{\bar{e}}^0 + (2 + \bar{s}_{12}^2)F_x^0. \end{aligned} \tag{30}$$

(v) *Pattern* P_{33}.—This case contains only CPT-violating patterns. In this case $p = |U_{e3}|^2 = s_{13}^2$ and $\bar{p} = |\bar{U}_{e3}|^2 = \bar{s}_{13}^2$. Then, the ν_e, $\bar{\nu}_e$, and ν_x spectra are given by

$$\begin{aligned} F_e &= s_{13}^2 F_e^0 + c_{13}^2 F_x^0 \approx F_x^0, \\ F_{\bar{e}} &= \bar{s}_{13}^2 F_e^0 + \bar{c}_{13}^2 F_x^0 \approx F_x^0, \\ 4F_x &= c_{13}^2 F_e^0 + \bar{c}_{13}^2 F_{\bar{e}}^0 + (2 + s_{13}^2 + \bar{s}_{13}^2)F_x^0 \\ &\approx F_e^0 + F_{\bar{e}}^0 + 2F_x^0. \end{aligned} \tag{31}$$

(vi) *Pattern* P_{22}.—This case contains only CPT-violating patterns. In this case $p = |U_{e2}|^2 = s_{12}^2 c_{13}^2$ and $\bar{p} = |\bar{U}_{e2}|^2 = \bar{s}_{12}^2\bar{c}_{13}^2$. Then, the ν_e, $\bar{\nu}_e$, and ν_x spectra are given by

$$\begin{aligned} F_e &= s_{12}^2 c_{13}^2 F_e^0 + (1 - s_{12}^2 c_{13}^2)F_x^0 \\ &\approx s_{12}^2 F_e^0 + c_{12}^2 F_x^0, \\ F_{\bar{e}} &= \bar{s}_{12}^2\bar{c}_{13}^2 F_{\bar{e}}^0 + (1 - \bar{s}_{12}^2\bar{c}_{13}^2)F_x^0 \\ &\approx \bar{s}_{12}^2 F_{\bar{e}}^0 + \bar{c}_{12}^2 F_x^0, \\ 4F_x &= (1 - s_{12}^2 c_{13}^2)F_e^0 + (1 - \bar{s}_{12}^2\bar{c}_{13}^2)F_{\bar{e}}^0 \\ &\quad + (2 + s_{12}^2 c_{13}^2 + \bar{s}_{12}^2\bar{c}_{13}^2)F_x^0 \\ &\approx c_{12}^2 F_e^0 + \bar{c}_{12}^2 F_{\bar{e}}^0 + (2 + s_{12}^2 + \bar{s}_{12}^2)F_x^0. \end{aligned} \tag{32}$$

VII. TO WHAT EXTENT CAN NEUTRINO FLUX PATTERNS BE DISCRIMINATED?

In this section, we briefly discuss to what extent the flux patterns predicted by six cases from P_{31} to P_{22} can be discriminated observationally. Our discussion cannot be a quantitative one because of the lack of a ''standard supernova model'' which has comparable accuracies possessed by the standard solar model. But, it may give us a feeling of how accurate should be the flavor-dependent reconstruction of neutrino spectra to discriminate the six different patterns of flavor conversion.

TABLE III. The parameters of the primary neutrino spectra models motivated from supernova simulations of the Garching (G1, G2) and the Livermore (L) groups, the same as used in [39]. We assume $\beta_{\nu_e} = 3.5$, $\beta_{\nu_x} = 4$, and $\beta_{\bar{\nu}_e} = 5$.

Model	$\langle E_0(\nu_e)\rangle$	$\langle E_0(\bar{\nu}_e)\rangle$	$\langle E_0(\nu_x)\rangle$	$\frac{\Phi_0(\nu_e)}{\Phi_0(\nu_x)}$	$\frac{\Phi_0(\bar{\nu}_e)}{\Phi_0(\nu_x)}$
L	12	15	24	2.0	1.6
G1	12	15	18	0.8	0.8
G2	12	15	15	0.5	0.5

We also address in Sec. VII C the question to what extent limiting the number of possible flux patterns by additional inputs helps in identifying CPT violation.

A. Model dependence of the prediction to flux spectral patterns

To reflect the best knowledge of supernova simulation currently at hand, we employ in this section the parametrization of fluxes which is used by the Garching group to fit their data [45,46]:

$$F^0_\alpha(E) = \frac{\Phi_\alpha}{\langle E_\alpha\rangle}\frac{\beta_\alpha^{\beta_\alpha}}{\Gamma(\beta_\alpha)}\left(\frac{E}{\langle E_\alpha\rangle}\right)^{\beta_\alpha - 1}\exp\left(-\beta_\alpha\frac{E}{\langle E_\alpha\rangle}\right), \quad (33)$$

where $\langle E_\alpha\rangle$ denotes their average energy, and β_α is a dimensionless parameter which is related to the width of the spectrum and typically takes on values 3.5–6. For definiteness, we assume $\beta_{\nu_e} = 3.5$, $\beta_{\nu_x} = 4$, and $\beta_{\bar{\nu}_e} = 5$. For the sake of comparison and to reveal dependence on supernova simulations we examine the three different sets of parameters, the same ones used in [39]. They are the fluxes obtained from the Livermore simulation [37] and the typical two model fluxes based on simulation done by the Garching group [47]. The three model flux parameters are given in Table III as L, G1, and G2.

In Fig. 4, the spectra of the three effective neutrino species ν_e, $\bar{\nu}_e$, and ν_x of six different patterns of P_{31} to P_{22} defined in (18) are plotted by taking model parameters G1 (upper figures) and G2 (lower figures) in Table III. As one can recognize the six flavor conversion patterns is much harder to distinguish than the case of the Livermore flux.

To obtain a hint on how much accuracy is needed to disentangle these six patterns we give in Table IV the averaged energies and width parameters of three species of neutrinos as done in Table II. With the Garching parameters, typically a few % accuracies for the determination of ratios $\langle E_\alpha\rangle/\langle E_{\bar{e}}\rangle$ and $\langle \Delta E_\alpha\rangle/\langle \Delta E_{\bar{e}}\rangle$ ($\alpha = e$ and x) are required. Whereas in the case of the Livermore parameters, we may be able to do the job with the accuracies of $\sim$10%.

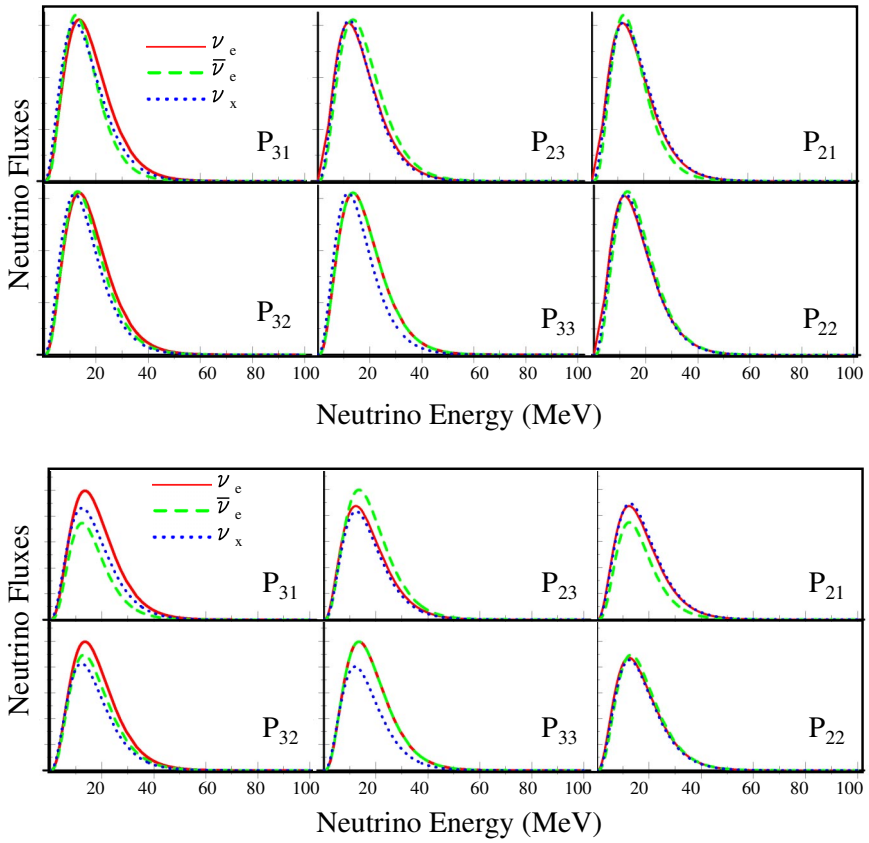

FIG. 4 (color online). The energy spectra of the three effective neutrino species ν_e (red solid curves), $\bar{\nu}_e$ (green dashed curves), and ν_x (blue dotted curves) at terrestrial detectors corresponding to six different patterns of neutrino flavor conversion P_{31} to P_{22} defined in (18) are presented. The Garching flux model parameters G1 (upper panels) and G2 (lower panels) are used.

TABLE IV. The same as in Table II but with the flux models G1 (upper table) and G2 (lower table) based on the Garching simulation with the parameters given in Table III. Two extra columns for luminosity ratios are added.

Spectral patterns	$\langle E_e\rangle$	$\langle E_{\bar e}\rangle$	$\langle E_x\rangle$	$\langle \Delta E_e\rangle$	$\langle \Delta E_{\bar e}\rangle$	$\langle \Delta E_x\rangle$	$\frac{\langle E_e\rangle}{\langle E_{\bar e}\rangle}$	$\frac{\langle E_x\rangle}{\langle E_{\bar e}\rangle}$	$\frac{\langle \Delta E_e\rangle}{\langle \Delta E_{\bar e}\rangle}$	$\frac{\langle \Delta E_x\rangle}{\langle \Delta E_{\bar e}\rangle}$	$\frac{\langle L_e\rangle}{\langle L_{\bar e}\rangle}$	$\frac{\langle L_x\rangle}{\langle L_{\bar e}\rangle}$
P_{31}	18.0	16.0	16.5	9.0	7.7	8.7	1.12	1.03	1.17	1.13	1.31	1.13
P_{23}	16.5	18.0	16.4	8.8	9.0	8.5	0.92	0.91	0.98	0.94	0.87	0.83
P_{21}	16.5	16.0	16.9	8.8	7.7	8.8	1.03	1.06	1.15	1.15	1.14	1.17
P_{32}	18.0	17.3	16.2	9.0	8.6	8.5	1.04	0.94	1.05	0.99	1.11	0.91
P_{33}	18.0	18.0	16.0	9.0	8.4	8.4	1.0	0.89	1.0	0.93	1.0	0.80
P_{22}	16.5	17.3	16.9	8.8	8.6	8.1	0.96	0.98	1.03	0.94	0.96	0.95

Spectral patterns	$\langle E_e\rangle$	$\langle E_{\bar e}\rangle$	$\langle E_x\rangle$	$\langle \Delta E_e\rangle$	$\langle \Delta E_{\bar e}\rangle$	$\langle \Delta E_x\rangle$	$\frac{\langle E_e\rangle}{\langle E_{\bar e}\rangle}$	$\frac{\langle E_x\rangle}{\langle E_{\bar e}\rangle}$	$\frac{\langle \Delta E_e\rangle}{\langle \Delta E_{\bar e}\rangle}$	$\frac{\langle \Delta E_x\rangle}{\langle \Delta E_{\bar e}\rangle}$	$\frac{\langle L_e\rangle}{\langle L_{\bar e}\rangle}$	$\frac{\langle L_x\rangle}{\langle L_{\bar e}\rangle}$
P_{31}	15.0	15.0	14.6	7.5	7.1	7.4	1.0	0.97	1.06	1.05	1.56	1.27
P_{23}	14.5	15.0	14.7	7.4	7.5	7.3	0.97	0.98	0.99	0.98	0.83	0.77
P_{21}	14.5	15.0	14.7	7.4	7.1	7.4	0.97	0.98	1.05	1.05	1.29	1.33
P_{32}	15.0	15.0	14.5	7.5	7.4	7.3	1.0	0.97	1.02	0.99	1.17	0.89
P_{33}	15.0	15.0	14.5	7.5	7.5	7.3	1.0	0.97	1.0	0.97	1.0	0.73
P_{22}	14.5	15.0	15.3	7.4	7.4	5.9	0.97	1.02	1.01	0.79	0.97	0.94

In addition to these quantities we have added in Table IV columns for the ratio of the luminosity of ν_e and ν_x to $\bar\nu_e$. (We note that even if the columns are added in Table II it is not informative because of the equipartition of luminosity between three species.) It should not be too difficult to distinguish among the six patterns if the luminosities are measured at the level of a few % level (G1) and 5%–10% level (G2).

B. How accurately can the supernova neutrino fluxes be determined?

We make a brief remark here to give the reader some feeling of how accurately the determination of the supernova neutrino fluxes can be done in a future observation of galactic supernovae. We must emphasize that the method for such flux reconstruction, which is of great importance solely from the supernova core diagnostics independent of testing CPT symmetry, is not yet developed to a sufficient level. It is the important problem that deserves a thorough study to identify a minimal set of detectors which are capable of reconstructing fluxes which can watch supernova for a long run of at least ~50 yr.

Lacking such studies we restrict ourselves to accuracy expected for parameters determinable with $\bar\nu_e$ observation in water Cherenkov detectors. In [38] it was found that the parameters of the primary flux $\langle E_{\bar e}\rangle$ and $\tau_E \equiv \langle E_x\rangle/\langle E_{\bar e}\rangle$ can be determined to the accuracies 1% (4%) and 1.5% (9%) at 3σ C.L. with Hyper-Kamiokande [48] (Super-Kamiokande), respectively. The accuracies found in [38] correspond to the ones of primary fluxes but we here assume that the similar accuracies can be expected for the terrestrial fluxes. If these accuracies can be extended to the ν_e flux (which is, however, highly nontrivial) it may be possible to disentangle the flux patterns expected in the six different patterns of flavor conversion. We stress that though the accuracy required for flux determination for identifying CPT violation is quite a demanding one, it is at the same level as that required to diagnose the interior of the supernova core by means of neutrinos.

C. How additional inputs from accelerator and reactor experiments help in identifying CPT violation

In Sec. V we have discussed which flux patterns will remain if the next generation accelerator and reactor experiments measure θ_{13} and $\bar\theta_{13}$ and/or determine the ν and $\bar\nu$ mass hierarchies. We discuss in this subsection how the reduction of numbers of possible flux patterns helps to discriminate between CPT invariant and noninvariant cases.

If the H level crossing is nonadiabatic, the two flux patterns P_{21} and P_{22} remain. In fact, it is the general feature of the nonadiabatic H level crossing, independent of mass hierarchy, as we have seen in Sec. V B. In the Garching flux model G1, the ratios of average neutrino energies and the widths of energy distributions of ν_e and ν_x to $\bar\nu_e$ are higher by about 7%–20% in the flux pattern P_{21} than in P_{22}. At the same time, the luminosity ratios are higher in P_{21} by about 20%. In the model G2, the luminosity ratios are again higher by 30%–40% in the flux pattern P_{21} than in P_{22}. The average energy and width ratios do not differ much except for $\langle \Delta E_x\rangle/\langle \Delta E_{\bar e}\rangle$ in which it is higher by about 30% in P_{21}.

If the H level crossing is adiabatic the results depend upon the ν and $\bar\nu$ mass hierarchies. If they are both normal we are left with two flux patterns P_{31} and P_{32} (Sec. V E). In the Garching flux model G1, all four ratios of average neutrino energies and their widths of the flux patterns P_{31}

are higher by about 10% than those of P_{32}. The luminosity ratios also differ by about 20%. In the model G2, average energy and width ratios do not show any appreciable difference, but the luminosity ratios are higher by 30%–40% in the flux pattern P_{31} than in P_{32}. If the ν and $\bar{\nu}$ mass hierarchies are both inverted there is no way of signaling CPT violation in our method.

Therefore, it appears that there is a chance to uncover CPT violation within the accuracy which may be expected in future detectors. Of course, we should not rely too much on the particular set of flux models to judge to what extent the different flux patterns are discriminable. But, the examination we have gone through in the above suggests that there are some possibilities of uncovering CPT violation by our method at least under circumstances helped by future terrestrial measurement.

D. Supernova model dependence

Here, we want to give a cautionary remark. Uncovering CPT violation along the way we discussed in this paper can be claimed only on the grounds that the supernova simulations at the time of observation are reliable to certain extent. Even in the luckiest case in which we know the mass hierarchy and that θ_{13} is in a region measurable by the next generation reactor and accelerator search, we need credibility in the flux model, roughly speaking, to 10%–20% level in the predictions to the ratios of average energy, width, and the luminosity of ν_e and ν_x to $\bar{\nu}_e$.

Suppose that a future measurement of supernova neutrino flux strongly suggests CPT violation by preferring one (or more) of the flux patterns which consists only of CPT-violating mass patterns, or by disfavoring any of the CPT invariant patterns. Then, one is tempted to conclude that CPT violation is signaled. The point is that the conclusion can be made firmer only by calibrating supernova simulation by the accumulation of data gained by many explosions for a consistency check. This point is an inherent weakness of the method of signaling CPT violation by supernova neutrino data. We want to emphasize, however, that it is quite thinkable that we will have a reliable model simulation of explosion in a timely way, by which neutrino flux can be predicted with high accuracies. Neutrinos are the main engine of the explosion (they are like the pp neutrinos in the sun) and, most probably, only the ordinary known physics is involved inside the core.

E. Implications to analyses with CPT invariance

As we mentioned at the end of Sec. I, part of the formulas and the analysis in this paper contain some information useful for conventional analysis with CPT, in particular, in the context of flavor-dependent reconstruction of three fluxes. We mention only a few points below, leaving full exposition to possible future works.

Look at the analytic formulas (27) and (28) in Sec. VI B. From these equations, we notice the following features: In (27) which applies to the case of normal mass hierarchy with adiabatic H resonance, the primary ν_e spectrum does not show up (or has a suppression factor of s^2_{13}) in the ν_e and $\bar{\nu}_e$ spectra observed at the terrestrial detectors. It means that to reconstruct the primary ν_e spectrum an accurate measurement of the ν_x spectrum together with those of ν_e and $\bar{\nu}_e$ is mandatory. Similarly, the primary $\bar{\nu}_e$ spectrum does not appear (or has a suppression factor of s^2_{13}) in the ν_e and $\bar{\nu}_e$ spectra in (28) which applies to the case of inverted mass hierarchy with adiabatic H resonance.

In these two cases it would be very difficult to reconstruct the primary ν_e ($\bar{\nu}_e$) spectrum in the case of normal (inverted) mass hierarchy with adiabatic H resonance, because a spectral measurement of ν_x is difficult. (See, however, [49] for a possible way out.) We believe that it is one of the crucial problems in the program of flavor-dependent reconstruction of primary neutrino fluxes in the interior of supernova.

The case of normal and inverted mass hierarchies with nonadiabatic H resonance, (29), may be the easiest one, relatively speaking, among the three CPT-conserving patterns. It is because a spectral measurement of $\bar{\nu}_e$ and ν_e (if possible) would allow us to determine all three primary fluxes if the separation of two Fermi-Dirac type distributions with different temperatures is possible, as illustrated in [38].

VIII. CONCLUDING REMARKS

We have discussed a method of using neutrinos from supernova to test CPT symmetry. Because of the possibility of having mass and mixing patterns of antineutrinos which can be different from neutrinos 32 different scenarios are allowed which differ in neutrino mass patterns and (non-)adiabaticity of high-density resonance. They produce six different patterns of supernova neutrino energy spectra at the terrestrial neutrino detectors, apart from a small modification due to the earth matter effect. Among the six patterns, three of them contain only the CPT-violating cases. Even in the mixed cases of CPT invariance and violation additional input on the values of θ_{13} from reactor and accelerator experiments further enhances the possibility of identifying CPT violation.

Future galactic supernovae watched by arrays of massive detectors may allow flavor-dependent reconstruction of three species of neutrino spectra, ν_e, $\bar{\nu}_e$, and ν_x (a collective notation for ν_μ, $\bar{\nu}_\mu$, ν_τ, and $\bar{\nu}_\tau$). Assuming capability of obtaining such information, which is also required to diagnose the supernova core in a conventional analysis with CPT, we have shown that one of the three CPT-violating patterns may be singled out observationally. Help by the other measurement of lepton mixing parameters by reactor and accelerator experiments would help to identify CPT-violating cases. Thus, we have shown that a

supernova neutrino can be a powerful tool to detect possible gross violation of CPT symmetry such as different mass patterns of neutrinos and antineutrinos. We emphasize the potential power of the method; it may allow one to disentangle different (1–3) and (1–2) mass hierarchies both in neutrino and antineutrino sectors in a single ''bang.''

However, we also noticed the weakness of the method. We have just mentioned the flux model dependence in the previous section. Another drawback of the method is a concern with its weakness at the precision test. In this paper, we have focused on the possibility of detecting CPT violation through identifying unequal mass patterns in neutrino and antineutrino sectors. If the two CPT violations in masses as well as mixing angles coexist, however, it would be very difficult to clearly distinguish the six different patterns of neutrino flavor conversion, the topics we are unable to address in this paper. Therefore, it is important to have a stringent bound on the difference between neutrino and antineutrino mixing angles in order for the supernova method for testing CPT to work. Similarly, the analysis would be very complicated if θ_{13} is in the intermediate region between adiabatic and nonadiabatic H resonance.

Suppose that CPT violation is signaled with supernova neutrinos in the way described in this paper. Then, one may feel that the confirmation by using a man-made neutrino beam is necessary because of the fundamental importance of CPT symmetry. Then, the question is, is it possible to confirm CPT violation by the alternative methods? Fortunately, the answer is yes. The possibility of using two detectors at the different baseline with the ν beam only (not $\bar{\nu}$) to determine the neutrino mass hierarchy has been proposed some time ago [50]. Therefore, a hypothesis of different mass hierarchies of neutrinos and antineutrinos can, in principle, be tested by a separate measurement using the π^+ and π^- beams. Determining the sign of Δm^2_{21} in the antineutrino sector is harder to carry out, as discussed in [27]. In any way, distinguishing neutrino mass hierarchy is a very challenging experiment and a large-scale apparatus is required. We emphasize, therefore, that the indication of CPT violation given by supernova neutrinos can give a good starting point for a vital search for the totally unexpected phenomenon of CPT violation.

ACKNOWLEDGMENTS

One of the authors (H. M.) thanks Hiroshi Nunokawa for discussions during a visit to the Departamento de Física, Pontifícia Universidade Católica do Rio de Janeiro, where this work was completed. This work was supported in part by the Grant-in-Aid for Scientific Research, No. 16340078, Japan Society for the Promotion of Science.

[1] S. Weinberg, *The Quantum Theory of Fields I* (Cambridge University Press, New York, 1995).
[2] S. Eidelman *et al.* (Particle Data Group Collaboration), Phys. Lett. B **592**, 1 (2004).
[3] A. Aguilar *et al.* (LSND Collaboration), Phys. Rev. D **64**, 112007 (2001). See, however, B. Armbruster *et al.* (KARMEN Collaboration), Phys. Rev. D **65**, 112001 (2002) for not completely consistent result.
[4] H. Murayama and T. Yanagida, Phys. Lett. B **520**, 263 (2001).
[5] Y. Fukuda *et al.* (Kamiokande Collaboration), Phys. Lett. B **335**, 237 (1994); Y. Fukuda *et al.* (Super-Kamiokande Collaboration), Phys. Rev. Lett. **81**, 1562 (1998); Y. Ashie *et al.* (Super-Kamiokande Collaboration), Phys. Rev. Lett. **93**, 101801 (2004); Y. Ashie *et al.* (Super-Kamiokande Collaboration), Phys. Rev. D **71**, 112005 (2005).
[6] B. T. Cleveland *et al.*, Astrophys. J. **496**, 505 (1998); J. N. Abdurashitov *et al.* (SAGE Collaboration), Phys. Rev. C **60**, 055801 (1999); W. Hampel *et al.* (GALLEX Collaboration), Phys. Lett. B **447**, 127 (1999); S. Fukuda *et al.* (Super-Kamiokande Collaboration), Phys. Lett. B **539**, 179 (2002); M. B. Smy *et al.* (Super-Kamiokande Collaboration), Phys. Rev. D **69**, 011104 (2004); Q. R. Ahmad *et al.* (SNO Collaboration), Phys. Rev. Lett. **87**, 071301 (2001); **89**, 011301 (2002); B. Aharmim *et al.* (SNO Collaboration), nucl-ex/0502021.
[7] K. Eguchi *et al.* (KamLAND Collaboration), Phys. Rev. Lett. **90**, 021802 (2003); T. Araki *et al.* (KamLAND Collaboration), Phys. Rev. Lett. **94**, 081801 (2005).
[8] M. H. Ahn *et al.* (K2K Collaboration), Phys. Rev. Lett. **90**, 041801 (2003); E. Aliu *et al.* (K2K Collaboration), Phys. Rev. Lett. **94**, 081802 (2005).
[9] G. Barenboim, L. Borissov, J. Lykken, and A. Y. Smirnov, J. High Energy Phys. 10 (2002) 001; G. Barenboim, L. Borissov, and J. Lykken, Phys. Lett. B **534**, 106 (2002); G. Barenboim, J. F. Beacom, L. Borissov, and B. Kayser, Phys. Lett. B **537**, 227 (2002); G. Barenboim and J. Lykken, Phys. Lett. B **554**, 73 (2003).
[10] A. Strumia, Phys. Lett. B **539**, 91 (2002).
[11] A. De Gouvea, Phys. Rev. D **66**, 076005 (2002).
[12] M. C. Gonzalez-Garcia, M. Maltoni, and T. Schwetz, Phys. Rev. D **68**, 053007 (2003).
[13] C. Saji (Super-Kamiokande Collaboration), in *Proceedings of the Fifth Workshop on Neutrino Oscillations and their Origin, Tokyo, Japan, 2004*, edited by Y. Suzuki, M. Nakahata, S. Moriyama, and Y. Koshio (World Scientific, Hackensack, 2005). p. 61.
[14] J. N. Bahcall, V. Barger, and D. Marfatia, Phys. Lett. B **534**, 120 (2002).
[15] H. Minakata, H. Nunokawa, W. J. C. Teves, and R.

Zukanovich Funchal, Phys. Rev. D **71**, 013005 (2005); Nucl. Phys. B, Proc. Suppl. **145**, 45 (2005).
[16] S. M. Bilenky, M. Freund, M. Lindner, T. Ohlsson, and W. Winter, Phys. Rev. D **65**, 073024 (2002).
[17] A. S. Dighe and A. Y. Smirnov, Phys. Rev. D **62**, 033007 (2000).
[18] See, e.g., J. F. Beacom, in Proceedings of the Neutrino Workshop at the Institute for Nuclear Theory, Seattle, Washington, 2000 (unpublished); H. Minakata, in Proceedings of the EuroConference on Neutrinos in the Universe, Lenggries, Germany, 2001 (unpublished).
[19] H. Minakata and H. Nunokawa, Phys. Lett. B **504**, 301 (2001).
[20] A. Y. Smirnov, D. N. Spergel, and J. N. Bahcall, Phys. Rev. D **49**, 1389 (1994).
[21] B. Jegerlehner, F. Neubig, and G. Raffelt, Phys. Rev. D **54**, 1194 (1996).
[22] V. Barger, D. Marfatia, and B. P. Wood, Phys. Lett. B **532**, 19 (2002).
[23] G. Raffelt (private communication).
[24] S. P. Mikheyev and A. Yu. Smirnov, Yad. Fiz. **42**, 1441 (1985) [Sov. J. Nucl. Phys. **42**, 913 (1985)]; Nuovo Cimento Soc. Ital. Fis. **9C**, 17 (1986); L. Wolfenstein, Phys. Rev. D **17**, 2369 (1978).
[25] Z. Maki, M. Nakagawa, and S. Sakata, Prog. Theor. Phys. **28**, 870 (1962). See also B. Pontecorvo, Zh. Eksp. Teor. Fiz. **53**, 1717 (1967) [Sov. Phys. JETP **26**, 984 (1968)].
[26] H. Minakata and H. Nunokawa, Phys. Rev. D **41**, 2976 (1990).
[27] A. de Gouvea and C. Pena-Garay, Phys. Rev. D **71**, 093002 (2005).
[28] Y. Itow *et al.*, hep-ex/0106019. An updated version can be found at http://neutrino.kek.jp/jhfnu/loi/loi.v2.030528.pdf
[29] D. Ayres *et al.* (Nova Collaboration), hep-ex/0503053.
[30] J. J. Gomez-Cadenas *et al.*, hep-ph/0105297.
[31] J. Burguet-Castell, D. Casper, E. Couce, J. J. Gomez-Cadenas, and P. Hernandez, Nucl. Phys. **B725**, 306 (2005).
[32] See, for example, H. Minakata, H. Sugiyama, O. Yasuda, K. Inoue, and F. Suekane, Phys. Rev. D **68**, 033017 (2003); **70**, 059901 (2004); K. Anderson *et al.*, hep-ex/0402041.
[33] C. Albright *et al.*, hep-ex/0008064; M. Apollonio *et al.*, hep-ph/0210192.
[34] M. Ishitsuka, T. Kajita, H. Minakata, and H. Nunokawa, Phys. Rev. D **72**, 033003 (2005); O. Mena Requejo, S. Palomares-Ruiz, and S. Pascoli, Phys. Rev. D **72**, 053002 (2005); K. Hagiwara, N. Okamura, and K. i. Senda, hep-ph/0504061.
[35] M. Nakahata, Nucl. Phys. B, Proc. Suppl. **145**, 23 (2005).
[36] A. Bandyopadhyay, S. Choubey, S. Goswami, and S. T. Petcov, Phys. Rev. D **72**, 033013 (2005).
[37] T. Totani, K. Sato, H. E. Dalhed, and J. R. Wilson, Astrophys. J. **496**, 216 (1998).
[38] H. Minakata, H. Nunokawa, R. Tomas, and J. W. F. Valle, Phys. Lett. B **542**, 239 (2002).
[39] R. Tomas, M. Kachelriess, G. Raffelt, A. Dighe, H. T. Janka, and L. Scheck, J. Cosmol. Astropart. Phys. 09 (2004) 015.
[40] C. Lunardini and A. Y. Smirnov, J. Cosmol. Astropart. Phys. 06 (2003) 009.
[41] G. Dutta, D. Indumathi, M. V. N. Murthy, and G. Rajasekaran, Phys. Rev. D **61**, 013009 (2000); G. Dutta, D. Indumathi, M. V. N. Murthy, and G. Rajasekaran, Phys. Rev. D **64**, 073011 (2001).
[42] K. Takahashi, M. Watanabe, K. Sato, and T. Totani, Phys. Rev. D **64**, 093004 (2001); K. Takahashi and K. Sato, Prog. Theor. Phys. **109**, 919 (2003).
[43] V. Barger, D. Marfatia, and B. P. Wood, Phys. Lett. B **547**, 37 (2002).
[44] C. Lunardini and A. Y. Smirnov, Nucl. Phys. **B616**, 307 (2001).
[45] M. T. Keil, Ph.D. thesis, TU München, 2003, astro-ph/0308228.
[46] M. T. Keil, G. G. Raffelt, and H. T. Janka, Astrophys. J. **590**, 971 (2003); G. G. Raffelt, M. T. Keil, R. Buras, H. T. Janka, and M. Rampp, astro-ph/0303226.
[47] R. Buras, H. T. Janka, M. T. Keil, G. G. Raffelt, and M. Rampp, Astrophys. J. **587**, 320 (2003).
[48] K. Nakamura, in Proceedings of the Next Generation of Nucleon Decay and Neutrino Detectors (NNN05), Aussois, Savoie, France, 2005 (unpublished).
[49] J. F. Beacom, W. M. Farr, and P. Vogel, Phys. Rev. D **66**, 033001 (2002).
[50] H. Minakata, H. Nunokawa, and S. J. Parke, Phys. Rev. D **68**, 013010 (2003); P. Huber, M. Lindner, and W. Winter, Nucl. Phys. **B654**, 3 (2003).